Antonina DOLGIH[1], Vladimir MARTEMYANOV[1], Valeriy BORIKOV[1]

Tomsk Polytechnic University, Russia (1)

doi:10.15199/48.2019.09.14

Dependence of the torque-rotor position characteristic from the tape winding current

Abstract. *The paper presents the results of numerical simulation of the torque motor with the novel active element representing the spirally wound conducting tape. The torque-rotor position characteristic of this motor is calculated using Comsol Multiphysics software and the obtained results are compared with the measurements on the experimental model of the torque motor with tape winding using the new methodology proposed.*

Streszczenie. *W artykule zaprezentowano wyniki symulacji numerycznej momentu silnika z nowym czynnym elementem w postaci spiralnej nawiniętej taśmy. Rezultaty obliczeń porównano z wynikami eksperymentalnymi na podstawie modelu silnika.* ***Zależność charakterystyki moment-pozycja wirnika w nowym rozwiązaniu silnika ze spiralnie nawiniętym uzwojeniem***

Keywords: torque motor, tape winding, torque-rotor position characteristic curve, experimental model, magnetic field.
Słowa kluczowe: moment silnika, taśmowe uzwojenie wirnika

Introduction

Permanent magnet torque motors have linear speed-torque and regulation characteristics, high operating speed, reliability and durability, especially in severe operation conditions. These advantages allow using permanent magnet torque motors in low-powered direct drives. At present, many companies are engaged in the development and improvement of such motors [1, 2]. The history, current state, main problems and solutions concerning torque motors, are described in the works of Mikerov [3-5]. Theoretical principles which are common practice in the operation of brushless DC torque motors are presented in [6-8]. Unlike classical motors, direct drive motors possess a modular structure consisting of two assemblies, namely rotor and stator. A rotor in a typical torque motor is made of high-coercivity rare-earth permanent magnets. A stator is made of laminated steel stacked up to carry windings. Steel laminations in stator can be slotted or slotless. A slotless core is more appropriate for high precision systems, since there is no cogging torque. In this design, permanent magnet motors are manufactured by industry [9-11]. Nowadays, both magnetic circuits and windings are being investigated in order to improve characteristics of torque motors [12, 13].

In 2008, a novel type of the torque motor active element was designed at Tomsk Polytechnic University. Thus, the traditional winding was replaced by a tape winding [14]. Benefits from this active element include the novel design and technological approach to the manufacture of the stator; a possibility of high current load with the appropriate heat removal; identification of desired functional dependence between the torque and rotor rotation angle.

Martemyanov and Dolgih [14] suggested a limited angle tape winding torque motor schematically presented in Fig. 1 [14]. The rotor represents a multipolar permanent magnet 1 connected to the magnetic core 2 via a non-magnetic disk 3. The stator 4 represents an active element comprising a spirally wound conducting tape coated with a layer of insulating material. At both lateral edges of the tape there are narrow transverse cuts arranged in turns. At each turn of the tape winding, these cuts locate above and under the similar cuts in underlying and overlying layers. These cuts form side slots on conducting tape. The distance between the adjacent slots corresponds to the polar pitch of the magnet. A DC source is connected to the ends of the wound tape.

The interaction between the quadrature current components and the permanent magnetic field results in forces, which, in turn, cause the torque moment. This moment rotates the magnetic system relative to the tape winding. Fig. 2 [14] presents a fragment of conducting tape. According to this figure, the current I has two components, namely: direct-axis component I_l along the tape and quadrature component I_t which crosses the tape in the direction coinciding with the rotor rotation axis. Rectangles N and S denote the magnet poles. The interaction between the quadrature component I_t and the magnetic field induces forces F acting on the magnet. The total action of these forces causes the torque that tends to turn the magnetic system relative to the stationary tape winding. The direct-axis components I_l induce forces P acting on suspension supports from the side of the magnet.

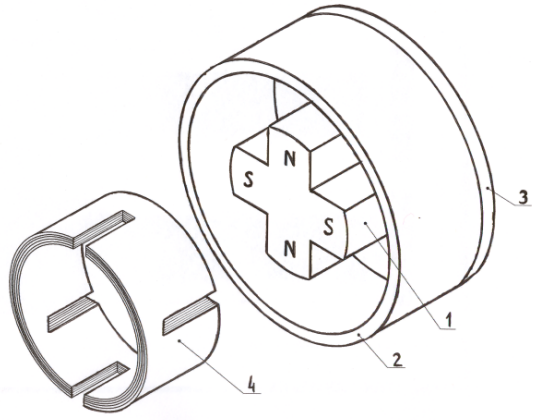

Fig.1. Schematic view of limited angle torque motor

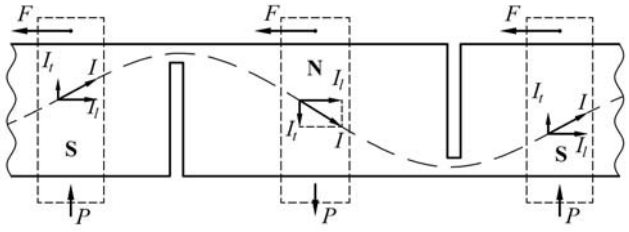

Fig.2. Schematic view of limited angle torque motor

The base parameters of the permanent torque motor include the torque curve which indicates the dependence $T=f(I)$ between the developed torque and the current in control winding and the torque-rotor position curve of $T(\alpha)$.

The torque curve is mostly linear [9, 11, 15, 16]. However, for the torque motor with tape winding [14] it may distort due to the influence of increased current of the tape

winding. This current creates a flux density that significantly distorts the main magnetic flux of the motor.

The torque-rotor position characteristic allows us to estimate the torque pulsation during the rotor rotation and the distortion of the main magnetic flux.

The purpose of this paper is to calculate the torque-rotor position characteristic in the motor with a novel active element using Comsol Multiphysics software and compare the obtained results with measurements on the experimental model of the torque motor with tape winding using the new methodology proposed.

Motor torque

Dolgih et al. [17] indicated that the torque of the tape winding motor is obtained from

$$T = B_\delta \cdot \frac{r_{av} \cdot \Delta}{I_0} \cdot \frac{U}{R} \cdot D(x, y, I_0). \tag{1}$$

In [18] they showed that at large currents the flux density depends on current $B_\delta(I)$.

If the motor torque is proportional to the winding current and depends on the flux density in the air gap, Eq. (1) can be written as

$$T = k_2 \cdot I \cdot \sum_{i=1,\, j=1}^{m,n} \left[D(x, y, I_0) \cdot B_\delta(I)\right]_{ij}. \tag{2}$$

Dolgih et al. [18] also suggested to divide the surface of the tape winding under the pole into $(m \cdot n)$ subdomains. In each ij subdomain the flux density is assumed to be constant and equals the average value of $(B_\delta)_{ij}$ for the given subdomain. At the same time, the double integral value of $\left[D(x, y, I_0)\right]_{ij}$ should also be detected for this subdomain.

Numerical simulation

Magnetic field of the pack of plates

The numerical simulation is carried out using Comsol Multiphysics software to show the curve distortion of the tape winding motor torque in occurrence of high currents. Figure 3 [18] illustrates the total current, which flows through the pack comprising 50 plates equals to (50*50) A.

Numerical calculations show that when the external magnetic field source is absent the magnetic field creates at diagonal current flow through the pack of plates as illustrated in Fig. 3 with red lines. The distribution of the flux density normal components is also shown in Fig. 3 with blue arrows [18].

Thus in this case, the generated magnetic field leads to a significant distortion of the main magnetic flux.

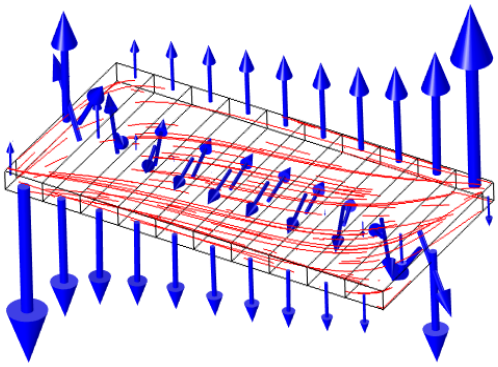

Fig.3. Magnetic field distribution

Magnetic field of tape winding

The model of the tape winding torque motor is designed in Comsol Multiphysics software. A parametric CAD software application T-FLEX CAD is used to design a 3D solid model of the torque motor presented in Fig. 4.

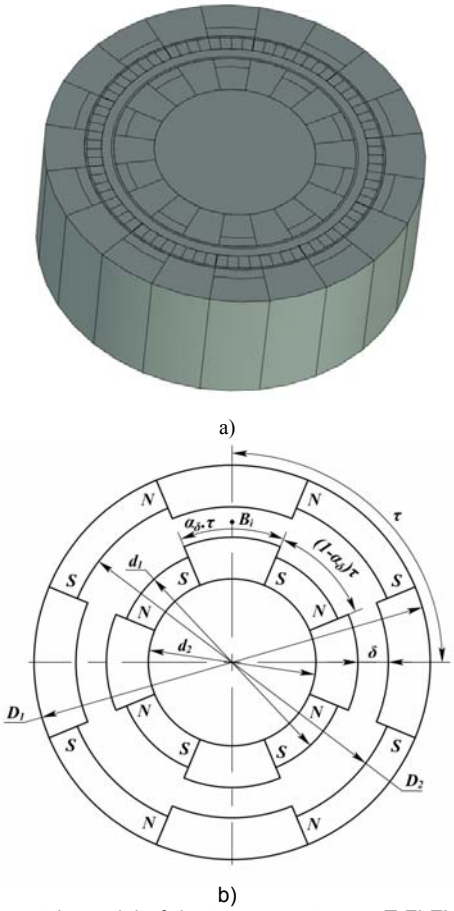

Fig.4. Parametric model of the torque motor: a - T-FLEX CAD 3D model; b - schematic view

Figure 5 [18] shows the fragment of the tape winding with the division into subdomains in which the flux density *B* is identified. This method simulates the rotation of the motor's magnetic system relative to the tape winding.

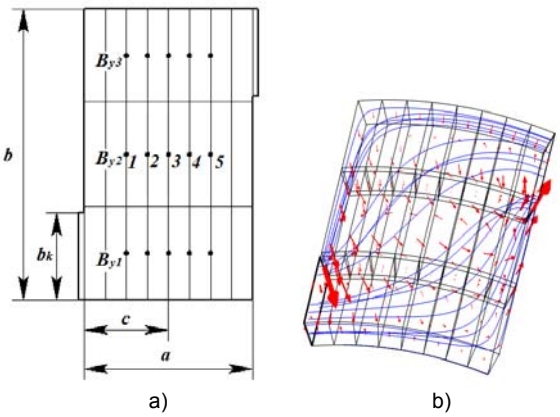

Fig.5. Schematic representation of the tape winding fragment: a – subdomains; b – flux density distribution

The distribution of the flux density is simulated according to three variants shown in Fig. 5a [18].

Variant I: Current flows through the tape winding. The magnetic circuit is absent.

Variant II: Current flows through the tape winding. The rotor is made of ferromagnetic material, without permanent magnets.

Variant III: Current flows through the tape winding. The rotor contains neodymium magnets and ferromagnetic poles.

Tables 1 and 2 summarize values of the magnetic flux density for the three variants and positions indicated in Fig. 5a. According to these tables, the total current which flows through the tape winding is 1250 and 2500 A, respectively.

Table 1. Magnetic flux density, I_{tot} = 1250 A

Pole position		1	2	3	4	5
B_{y1}, T	I	0.002	0.008	0.013	0.017	0.023
	II	0.068	0.083	0.099	0.114	0.128
	III	-0.308	-0.301	-0.294	-0.286	-0.278
B_{y2}, T	I	-0.030	-0.013	$2 \cdot 10^{-5}$	0.013	0.030
	II	-0.073	-0.035	$-5 \cdot 10^{-5}$	0.035	0.073
	III	-0.450	-0.421	-0.393	-0.365	-0.334
B_{y3}, T	I	-0.023	-0.017	-0.013	-0.008	-0.002
	II	-0.128	-0.114	-0.099	-0.084	-0.068
	III	-0.503	-0.497	-0.491	-0.482	-0.473

Table 2. Magnetic flux density, I_{tot} = 2500 A

Pole position		1	2	3	4	5
B_{y1}, T	I	0.004	0.016	0.025	0.035	0.045
	II	0.136	0.167	0.198	0.227	0.256
	III	-0.233	-0.213	-0.197	-0.182	-0.166
B_{y2}, T	I	-0.059	-0.026	$4 \cdot 10^{-5}$	0.027	0.060
	II	-0.147	-0.071	$-1 \cdot 10^{-4}$	0.071	0.146
	III	-0.514	-0.450	-0.394	-0.339	-0.276
B_{y3}, T	I	-0.045	-0.095	-0.026	-0.016	-0.004
	II	-0.257	-0.227	-0.199	-0.167	-0.136
	III	-0.617	-0.601	-0.588	-0.570	-0.551

If the current does not flow through the tape winding, the magnetic flux of the motor is uniform and the flux density is about 0.4 T. If the current flows through the tape winding (Variant III), the main magnetic flux distorts. Figure 6 presents the resulting density distributions 1 and 5 of magnetic flux.

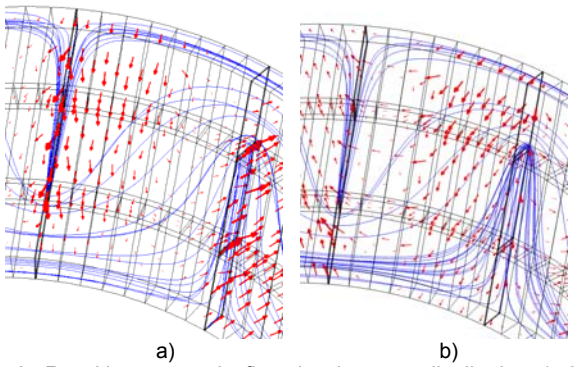

a) b)

Fig. 6. Resulting magnetic flux density: a – distribution 1; b – distribution 5

The simulation results allow us to determine the distribution of the flux density in the air gap. These results can be obtained at different pole positions relative to tape winding pack. We selected five such positions.

Torque-rotor position characteristic for limited angle torque motor

According to Eq. (2), numerical simulations (Tables 1 and 2), and values of the double integral previously obtained for each of selected subdomains of the tape winding pack, we can derive the developed torques for the five selected rotor positions. Figure 7 [18] plots dependences between two values of the total current flows. Curves 1 and 3 do not show the impact of control current, which flows through the tape winding, whereas curves 2 and 4 indicate this impact.

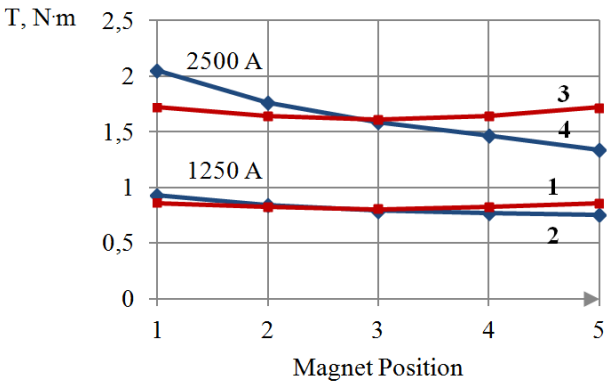

Fig.7. Torque-rotor position characteristics

Torque-rotor position characteristic for brushless DC torque motor

The proposed idea can be readily used in a two-phase brushless DC (BLDC) motor designed similar to the limited angle torque motor (see Fig. 1) using two tape windings. The cuts of the second tape winding are shifted relative to the first tape winding by a half of the polar pitch.

In this variant, the torque combined characteristic has no zero points. If the torque dependences of both windings are identical and represent a combination of isosceles triangles, the resulting motor torque is unchanged for each of the rotor positions. Ideally, the torque pulsation is absent (Fig. 8).

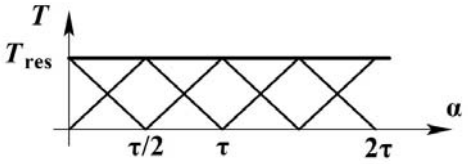

Fig.8. Two-phase BLDC motor torque V-shaped dependence between the torque and rotor rotation angle

V-shaped dependence between the torque and rotor rotation angle can be obtained with only two additional cuts on each plate of the tape winding (Fig. 9).

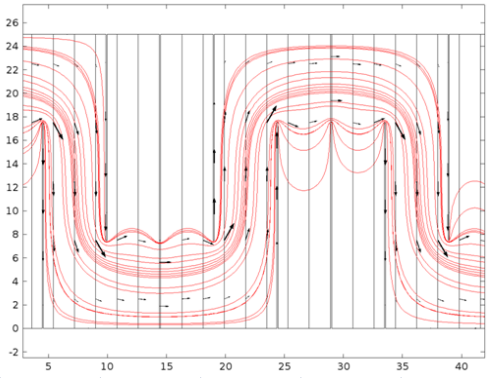

Fig.9. Tape winding view with two additional cuts

In order to obtain V-shaped dependence, the tape winding design was modified with two additional cuts in each plate in the parametric T-FLEX CAD 3D model of the torque motor shown in Fig. 4a. As a result of numerical simulation described earlier in this paper, resulting torque-rotor position curves are suggested with and without the impact of the tape winding current (Fig. 10).

Torque measurement technique

The experimental unit is designed to confirm the results of numerical simulation. Its full view is illustrated in Fig. 11. The unit comprises a tape winding torque motor with a loading device, a power source, and a contact sensor which detects the point where the motor torque equals the load torque.

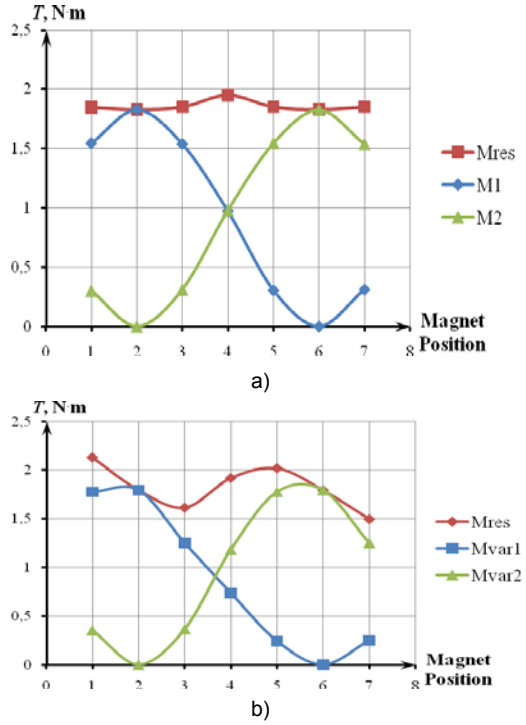

Fig.10 Resulting torque-rotor position characteristics: *a* - without the impact of tape winding current; *b* - with the impact of tape winding current

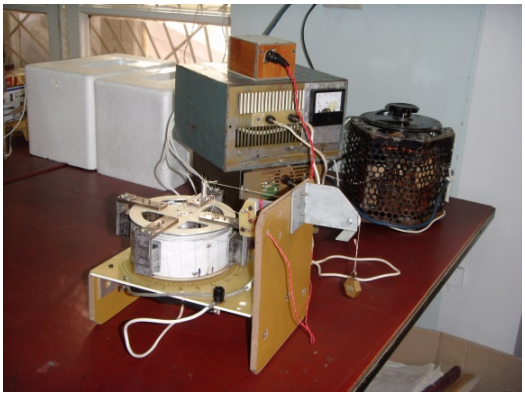

Fig.11. Experimental unit

The model of the torque motor presented in Fig. 12 is placed on a dielectric base. The design is such to rotate the stator around the rotor which is positioned relative to the base due to the operating principle of the contact sensor. To ensure the relative position of the stator and rotor, the scale on the base is used. Once the stator is positioned, it is fixed to the base with clamping screws. The torque measurement technique is as follows. The tape winding placed on the stator is supplied with direct current slowly varying from zero to the value, when the contact sensor responds. This means that the motor torque overcomes the load torque. This current value is recorded and used to determine the motor characteristics. In our experiment, the current does not exceed 5 A.

Figure 12a shows the process of the load torque creation using a suspended calibrated weight, the thread being connected with the rotor on the master arm. The load torque enables the electrical contact between the rotor and the base. The main model elements are illustrated in Fig. 12b. Tape winding 1 is made of aluminum tape 0.07 mm thick with one side isolated with paper. The tape is wound on a thin glass made of anodized aluminum. The winding consists of 70 turns with four sections in each which relate to the polar pitch. As can be seen from Fig. 12b, the rotor magnetic system 2 consists of four pairs of rare-earth permanent magnets. The real air gap is 20 mm. The flux density is 0.06 T. The rotor suspension assembly 3 is made on ball bearings.

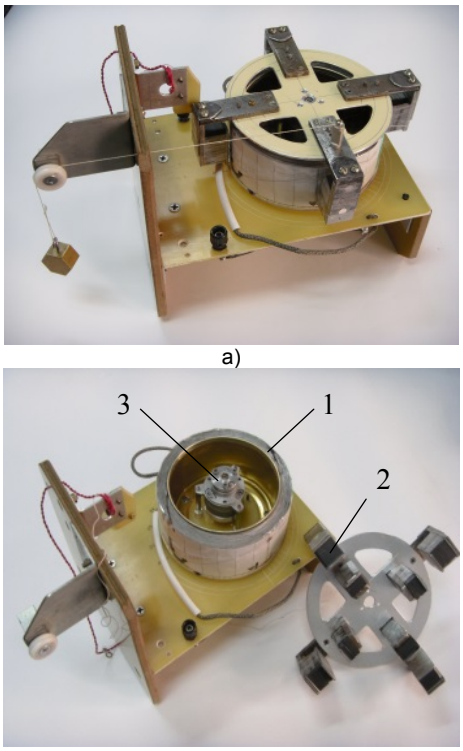

Fig.12 The torque motor model: *a* - load torque creation process; *b* - main elements

The linear dependence of the developed torque allows us to obtain a torque-rotor position characteristic at a current of 1 A which flows through the tape winding. Figure 13 plots this characteristic for a single tape turn.

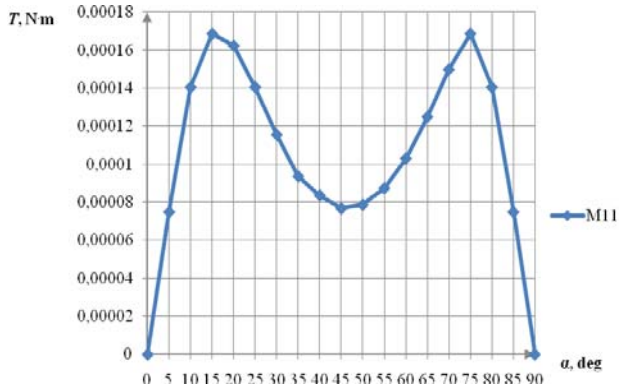

Fig.13. Experimental torque-rotor position characteristic

Conclusions

Based on the results, it can be concluded that despite the similarity of the proposed torque motor with the permanent magnet to motors used in practice, a particular

methodology and research tools should be developed. As a first approximation, the static torque measurements were carried out using the new method proposed. The torque pulsation can be detected by the same method depending on the rotor angle of rotation, however, the quality of the experimental model should be improved. Measurements of the conducting tape are not so difficult. Particular attention should be paid to a possible Hall effect which can modify the behavior of line currents in the tape winding, thereby changing the double integral and torque values. The suggested numerical model does not describe the Hall effect. Therefore, a highly sensitive experimental model should be developed to compare experimental data and numerical calculations with the use of correction factors.

The research is carried out at Tomsk Polytechnic University within the framework of Tomsk Polytechnic University Competitiveness Enhancement Program grant.

***Authors**: associate prof. Ph.D. Antonina Dolgih, Tomsk Polytechnic University, School of Non-Destructive Testing, 30 Lenin avenue, 634050 Tomsk, Russia, E-mail: ivanovatonya@tpu.ru; associate prof. Ph.D. Vladimir Martemyanov, Tomsk Polytechnic University, School of Non-Destructive Testing, 30 Lenin avenue, 634050 Tomsk, Russia, E-mail: martemjanov@tpu.ru; prof. dr. Valeriy Borikov, Tomsk Polytechnic University, School of Non-Destructive Testing, 30 Lenin avenue, 634050 Tomsk, Russia, E-mail: borikov@tpu.ru.*

REFERENCES

[1] *INA – Drives & Mechatronics. Brochure* (GmbH & Co. KG, IDAM Direct Drives, 2014)
[2] *About ETEL Torque Motors. Catalog. Torque motors handbook* 2017
http://www.etel.ch/fileadmin/ PDF/Catalogs/ Torque_Motors/Torque_Motors_V2.0_english.pdf.
[3] Dubrovskiy G, Mikerov A, Dzhankhotov V and Pyrhonen J 2014 General comparison of direct and geared drives for control applications *EPE-ECCE Europe* 6910754
[4] Astakhov D A, Mikerov A G and Yakovlev A V 1993 A contactless torque drive for social and biomedical equipment *Elektrotekhnika* **7** 17-9
[5] Mikerov A G 2009 Brushless DC torque motors quality level indexes for servo drive applications *IEEE EUROCON 2009* 5167730 827-34
[6] Hanselman D 2006 *Brushless Permanent Magnet Motor Design. Second Edition* (Magna Physics Publishing, United States of America)
[7] Hughes A and Drury B 2013 *Electric Motors and Drives. Fundamentals, Types and Applications. 4th Edition* (Elsevier-Newnes, Oxford)
[8] Madaan P 2013 *Brushless DC Motors. Part 1. Construction and Operating Principles* (Cypress Semiconductor, India)
[9] Gieras J F 2010 *Permanent Magnet Motor Technology: Design and Applications*, *3rd ed.* (CRC Press) p 328
[10] Sedgewick R D 1982 Zig-zag windings, winding machine, and method *US Patent* № 4331896 A
[11] *Technical information, 2d ed* 2016 (Dr. Fritz Faulhaber GmbH & Co. KG) p 71
[12] Zhu Z Q and Howe D 2000 Influence of design parameters on cogging torque in permanent magnet machines *IEEE Transactions on Energy Conversion* **15** 407-12
[13] Zhu L, Jiang S Z, Zhu Z Q and Chan C C 2009 Analytical methods for minimizing cogging torque in permanent-magnet machines *IEEE Transactions on Magnetics* **45(4)** 2023-31
[14] Martemjanov V and Dolgih (Ivanova) A 2012 Torque motor *RF Patent* № 2441310
[15] Crowder R 2006 *Electric Drives and Electromechanical Systems: Applications and Control* (Elsevier Science & Technology Books, London)
[16] Tsai C C, Lin S C, Huang H C and Cheng Y M 2009 Design and control of a brushless DC limited-angle torque motor with its application to fuel control of small-scale gas turbine engines *Mechatronics* **19** 29-41
[17] Dolgih A, Martemyanov V and Samodurov I 2016 Analytical studies of torque motor tape active element *MATEC Web of Conf.* **48** 01004 DOI: 10.1051/confmatec/20164801004
[18] Dolgih A, Martemyanov V and Samodurov I 2017 The tape winding current impact on the motor's torque curve *MATEC Web of Conferences* **102** 01014 DOI: 10.1051/matecconf/201710201014